Title: Remodelling of human bone on the chorioallantoic membrane (CAM) of the chicken egg: *De novo* bone formation and resorption

Running title: Human bone formation within a novel *in vivo* chick assay

Authors: Inés Moreno-Jiménez[1], Stuart A. Lanham[1], Janos M. Kanczler[1], Gry Hulsart-Billstrom[1], Nicholas D. Evans[1] and Richard OC Oreffo*[1].

Email address: I.Moreno@soton.ac.uk; S.A.Lanham@soton.ac.uk; J.Kanczler@soton.ac.uk; S.Hulsart-Billstrom@soton.ac.uk; N.D.Evans@soton.ac.uk; Richard.Oreffo@soton.ac.uk

Bone and Joint Research Group, [1]Centre for Human Development, Stem Cells and Regeneration, Human Development and Health, Institute of Developmental Sciences University of Southampton, Tremona Road, Southampton, SO16 6YD, UK

*Corresponding author Richard OC Oreffo; Faculty of Medicine University of Southampton Institute of Developmental Sciences Building Mailpoint 887 Southampton General Hospital Tremona Road Southampton SO16 6YD Tel: +44 (0)23 8120 8502; Email: richard.oreffo@soton.ac.uk

Keywords: human bone; chorioallantoic membrane (CAM assay); micro computed tomography (μCT); 3D registration, *in vivo*; tissue engineering; BMP2, preclinical model.

This article has been accepted for publication and undergone full peer review but has not been through the copyediting, typesetting, pagination and proofreading process which may lead to differences between this version and the Version of Record. Please cite this article as doi: 10.1002/term.2711

Abstract

Traditionally used as an angiogenic assay, the chorioallantoic membrane (CAM) assay of the chick embryo offers significant potential as an *in vivo* model for xenograft organ-culture. Viable human bone can be cultivated on the CAM and increases in bone volume are evident, however, it remains unclear by what mechanism this change occurs and whether this reflects the physiological process of bone remodelling. In this study we tested the hypothesis that CAM-induced bone remodelling is a consequence of host and graft mediated processes. Bone cylinders harvested from femoral heads post-surgery were placed on the CAM of GFP-chick embryos for 9 days, followed by micro-computed tomography (μCT) and histologically. 3D registration of consecutive μCT-scans showed newly mineralised tissue in CAM-implanted bone cylinders, as well as new osteoid deposition histologically. Immunohistochemistry demonstrated the presence of bone resorption and formation markers (Cathepsin K, SOX9 and RUNX2) co-localising with GFP staining, expressed in avian cells only. To investigate the role of the human cells in the process of bone formation, decellularised bone cylinders were implanted on the CAM and comparable increases in bone volume were observed, indicating that avian cells were responsible for the bone mineralisation process. Finally, CAM implantation of acellular collagen sponges, containing BMP2, resulted in the deposition of extracellular matrix and tissue mineralisation. These studies indicate that the CAM can respond to osteogenic stimuli and support formation/resorption of implanted human bone; providing a humanised CAM model for regenerative medicine research and a novel short-term *in vivo* model for tissue engineering and biomaterial testing.

Introduction

For over a century, the chorioallantoic membrane (CAM) of the chicken (*Gallus gallus domesticus*) egg has provided an *ex vivo* bioincubator for the engraftment of test compounds or materials (Rous and Murphy, 1911). The CAM develops from the fusion of the chorion and the allantois around day 4 of the 21-day incubation period of the chick and continues to develop until day 14. The primary function of this extraembryonic membrane is to serve as a respiratory organ, providing the O_2/CO_2 gas exchange between the eggshell and the chick embryo during the gestational process (Nowak-Sliwinska, Segura and Iruela-Arispe, 2014). Although traditionally used as an angiogenic assay due to the rapid growth of the CAM capillaries (Ribatti *et al.*, 2006; Kilarski *et al.*, 2012), the applications of the CAM assay have expanded into multiple fields, including biocompatibility evaluation of biomaterials and organ culture (Kanczler *et al.*, 2007; Keshaw *et al.*, 2010; Baiguera, Macchiarini and Ribatti, 2012; Lee *et al.*, 2015). Importantly, the CAM is a non-innervated and highly vascularised structure and for this reason has been exploited as a surrogate blood supply for any engrafted construct (Nowak-Sliwinska, Segura and Iruela-Arispe, 2014; Moreno-Jimenez *et al.*, 2017).

Moreover, due to the undeveloped immune system of the chick embryo, the CAM has been used for xenograft culture of a variety of organs (brain, aorta, skin, etc.) of different species (murine, human, avian, etc.)(Murphy, 1913; Kunzi-Rapp, Rück and Kaufmann, 1999; Stallmach *et al.*, 2001; Ribatti *et al.*, 2003; Coconi *et al.*, 2005; Lokman *et al.*, 2012). The CAM has also been used as an *ex vivo* bioreactor for viable tissue such as neonatal mouse skin, where the appearance of the graft, following implantation (pink and healthy *versus* necrotic), was used to evaluate transplantation success (Carre *et al.*, 2012). The authors induced a laser-wound on the skin grafts following CAM-implantation and showed complete, scarless healing within 4 days of *in vivo* culture (Carre *et al.*, 2012). Additional studies have described vascularisation and CAM-integration of human derived viable tissue, including skin, placenta and ovarian tissue (Kunzi-Rapp, Rück and Kaufmann, 1999; Stallmach *et al.*, 2001; Martinez-Madrid *et al.*, 2009; Carre *et al.*, 2012).

The chicken embryo has a long history as an *in vivo* model for skeletal development. As early as 1946, Hancox implanted chick calvarial bone fragments on the CAM to examine the mechanism of bone

transplant survival (Hancox, 1946). Maeda and Noda used flat X-rays to compare growth of chick femurs cultured *in vivo* (CAM) or *in vitro* for an equivalent incubation period, showing a significant increase in length and diameter when CAM-implanted for 6 days (Maeda and Noda, 2003). The same study evaluated the role of the perichondrium in the bone formation process, and noted differences only when the bone organs were implanted on CAM and not following *in vitro* culture (Maeda and Noda, 2003). In addition to bone formation, bone resorption has also been demonstrated on the CAM of the chicken embryo (Webber, Menton and Osdoby, 1990; Collin-Osdoby *et al.*, 2000). For example, bovine cortical bone chips were CAM-implanted and showed bone resorption pits as early as 3 days post grafting (Collin-Osdoby *et al.*, 2000). This experimental setup was also used to evaluate the role of a nitric oxide inhibitor on osteoclast activity and demonstrated higher numbers of bone resorption pits and Tartrate-resistant acid phosphatase (TRAP) activity compared to control samples (Collin-Osdoby *et al.*, 2000). The CAM assay has also been used to evaluate materials for their use in the field of tissue engineering. Takahashi *et al*. examined the healing process of a chick femoral bone defect on the CAM over 9 days, and demonstrated matrix deposition from day 5 and full regeneration from day 7 (Takahashi *et al.*, 1991). Similarly, Yang *et al*. tested the potential of a porous polymer biomaterial scaffold releasing bone morphogenetic protein 2 (BMP2) using a chick femoral wedge-defect model and the CAM assay as a bioreactor, and reported complete defect bridging of the femur (Yang *et al.*, 2004).

Current efforts within animal research, particularly within the regenerative medicine field, are centred on conducting high quality science while reducing use and improving the welfare of laboratory animals (Russel, W. M. S and Burch, 1959). In this context, we have shown that the CAM assay of the developing chick embryo can serve as a short term, simple, cost-effective and, importantly, less sentient *in vivo* model for biomaterial assessment (Yang *et al.*, 2004; Kanczler *et al.*, 2007; Moreno-Jimenez *et al.*, 2017). These studies demonstrate the ability of the CAM to integrate xenograft tissue and in particular, for bone, allow for osteogenic processess (formation and resorption) to occur in the context of blood vessel supply. This offers a significant advantage over *in vitro* culture models (*i.e.* organotypic) as bone tissue regeneration is critically dependent on angiogenesis (Kanczler and Oreffo,

2008). Furthermore, the culture of bone tissue using the CAM assay could serve as an attractive short-term alternative to more invasive and technically demanding *in vivo* models (*e.g.* murine subcutananous implant) for the evaluation of novel biomaterials for regenerative medicine. This has the benefits of increasing the number of experimental replicates in a study at little financial cost, and reducing and refining the use of sentient animal models in biomedical research. Moreover, the opportunity to culture human bone tissue on the CAM (*i.e.* humanised CAM model) would provide a more clinically relevant scenario to allow for novel treatment screening (Xiao *et al.*, 2015). Indeed, recent advances in the field of regenerative medicine and cancer-metastasis research are moving towards the implementation of humanised models for preclinical research (Ito *et al.*, 2012; Holzapfel *et al.*, 2015; Xiao *et al.*, 2015).

Exploiting this prospective, we have previously demonstrated a novel method to culture viable human bone tissue (cylinders) on the CAM (Moreno-Jiménez *et al.*, 2016). In contrast to the human bone tissue cultured *in vitro*, CAM-implanted bone cylinders showed the presence of avian blood vessels, condensations of progenitor (SOX9+) cells, extracellular matrix deposition, and significant increase in bone volume (Moreno-Jiménez *et al.*, 2016). Moreover, human bone autologous cells remained viable following CAM-implantation (Moreno-Jiménez *et al.*, 2016). However, in this previous study (Moreno-Jiménez *et al.*, 2016), we were unable to identify the mechanisms involved in the bone formation.

In this study, we hypothesise that CAM-implantation of human bone cylinders promotes active bone remodelling, in addition to the *de novo* formation of ectopic bone. To test this, we employed a combination of high resolution micro computed tomography (µCT) and histological techniques to determine the location and origin of the formed bone. Given the dynamic nature of bone, in which changes can include both bone deposition and bone resorption, there is a need to find new approaches focused on uncoupling both processes from a single output (*i.e.* µCT scan). Superposition of two or more sequential scans (3D registration) to separately identify the areas of bone formation and resorption, has been described in several studies (Waarsing *et al.*, 2004; Schulte *et al.*, 2011; Birkhold *et al.*, 2014). Importantly, this approach would bypass the inability to differentiate pre-existing bone

from newly formed mineralised tissue on CAM-implanted bone cylinders. The current study has validated the CAM as a humanised, short-term *in vivo* culture system to study bone regeneration and tissue repair, providing an intermediate model between *in vitro* and *in vivo* in the pipeline of preclinical research for biomaterial testing.

Results

Aims and experimental design

In previous work, we developed a method to culture viable human bone cylinders *in vivo* using the CAM assay, and showed a significant increase in bone volume as well as viability of the human autologous cells following implantation (Moreno-Jiménez *et al.*, 2016). To investigate the mechanism behind these effects, we used the CAM assay from genetically modified chicken embryos, which expressed green fluorescent protein (GFP), as a short term *in vivo* model to examine bone formation (Figure 1 A). In brief, bone cylinders were freshly isolated from a human femoral head (Figure 1 Ai) and prepared for a 9 day incubation period on CAM (Figure 1 Aiii), or maintained using *in vitro* culture as controls. Before and after incubation, bone cylinders were individually scanned using µCT to examine changes in bone resorption/formation within the cylinder (Figure 1 A ii, v, vi). Furthermore, to identify the mechanism of bone formation and to examine the CAM assay as an ectopic model of bone formation (Figure 1 B), commercial acellular collagen sponges (ACS) containing ± 2.4 µg BMP2 were implanted on the CAM for the same period, followed by µCT analysis and mineralised tissue assessment.

Identification of newly deposited and resorbed bone in human bone cylinders following CAM-implantation

Using our previously published protocol (Moreno-Jiménez *et al.*, 2016), we implanted freshly-isolated human bone cylinders on the CAM and were able to measure increases in bone volume following incubation. CAM-implanted bone cylinders displayed a significant increase (9.79 % ± 2.24 SD; n=6-8; $p<0.001$) compared to *in vitro*-cultured bone cylinders (1.60 % ± 1.06 SD) and control (-0.19 % ± 0.33 SD; bone cylinders maintained at 4°C) from the same donor. To identify the location of the newly formed bone, 3D registration was conducted on the pre- and post-scans of the human bone cylinders that had been implanted on the CAM, cultured *in vitro* or maintained at 4°C (internal control) for 9 days. In short, 3D registration allowed for consecutive (pre and post incubation) scans to be superposed and, once aligned, subtraction of one from another to identify the positive (purple) and negative (green) differences (Figure 2 A, for more details on this method see Supplementary Figure 1). Positive (Figure 2 C, H, M) and negative (Figure 2 B, G, L) differences were coloured purple and green respectively, and merged for comparison in each condition (Figure 2 D, I, N). In addition, the histograms in greyscale of the positive and negative difference were plotted (Figure 2 E, J, O), or subtracted from one another (Figure 2 F, K, P). A reproducibility control was included to validate the registration technique (Supplementary Figure 2 A-E) as well as a negative control to show bone loss following decalcification (Supplementary Figure 2 F-J). Note that even following a strong decalcification protocol, there were still a significant number of voxels in the positive difference channel (see Supplementary Figure 2 G, I). Despite this, there was always a significantly greater number of voxels in the negative channel; indicating significant demineralisation. The presence of voxels in the positive channel reflects the accuracy within the 3D registration procedure, which iteratively fits one scan to another, and thus is more accurate when comparable, untreated, samples are used (compare Supplementary Figure 2 A and B).

Bone cylinders from the same femoral head were maintained at 4°C during the equivalent incubation period (control group) as a baseline reference to test the alignment precision for each experiment. The control group showed a minimal number of voxels in both positive and negative channels (Figure 2 B-

D), following subtraction from each other (Figure 2 F, E). Similarly, *in vitro* treatment showed a comparable fraction of positive and negative voxels (Figure 2 G-I), again showing minimal variance after subtraction (Figure 5 J-K). In contrast, CAM-implanted bone cylinders showed a greater proportion of positive over negative voxels in the 3D images (Figure 2 L-N), further evidenced by a positive net change (+ 2.4 mm^3) following subtraction (Figure 2 O, P). In agreement our previous study, quantification of the whole cylinder bone volume pre and post incubation showed a +8.13 % change in CAM-implanted samples, compared to - 0.26 % and - 0.11 % for the control and *in vitro* samples, respectively. These results support the conclusion that newly formed bone in the cylinders can be visualised and localised using 3D registration on consecutive scans.

Bone remodelling (osteoid deposition and bone resorption) occurs in human bone cylinders after CAM-implantation

Next, we analysed histologically the increased bone volume of CAM-implanted bone cylinders detected on µCT analysis. After incubation, *in vitro*-cultured and CAM-implanted bone cylinders were processed for mineralised tissue histochemistry to enable distinction between mineralised tissue (green) and newly deposited osteoid (red) using Goldner's Trichrome staining (Figure 3). CAM-implanted bone cylinders showed osteoid deposition at the edges of the trabecular bone (Figure 3 A-C), particularly in the regions in close proximity to the CAM (see red arrows Figure 3 B). Cuboidal-shaped cells appeared aligned with the newly deposited osteoid in the CAM-implanted bone cylinders, indicative of osteoblastic cells (see black arrows Figure 3 C). In contrast, negligible osteoid was observed within the *in vitro*-cultured bone cylinders (Figure 3 D-F). Hence, histology demonstrated the presence of new osteoid deposition within the CAM-implanted bone cylinders compared to *in vitro*-cultured group.

To evaluate whether the CAM was able to elicit bone resorption as well as bone formation, human bone cylinders were cultured *in vitro* or on the CAM of genetically modified chick embryos expressing GFP, and examined for osteoclast activity. Positive immunostaining for Cathepsin K, a marker of osteoclast resorption, was present around trabecular bone debris on CAM-implanted

cylinders (see arrows Figure 4 A-B). This finding was consistent, across independent experiments, using different donor sources of bone.

Moreover, immunostaining on consecutive sections indicated co-localisation of the osteoclast marker around trabecular bone spicules with GFP expression, only present in avian cells (see arrows Figure 4 C). *In vitro*-cultured bone cylinders showed no expression of Cathepsin K or GFP on trabecular bone and marrow (Figure 4 E-F). Overall, this data demonstrated that viable human bone cylinders undergo osteoid deposition and matrix resorption by osteoclast cells, likely to be of avian origin, following short-term *in vivo* implantation on CAM.

Avian cells form endochondral (SOX9+/RUNX2+) cell condensations and drive the increase in bone volume of human bone cylinders following CAM-implantation.

Histological evaluation of the CAM-integrated bone cylinders showed the presence of the avian membrane encapsulating the human bone tissue with numerous blood vessels evident (see arrows Supplementary Figure 3). In addition to extracellular matrix deposition, CAM-implanted bone cylinders showed the presence of multiple cell condensations at the interface between human and avian tissue (see asterisks in Supplementary Figure 3). To identify the developmental origin of these cell condensations, immunohistochemistry for chondrogenic (SOX9) and osteogenic (RUNX2) transcription factors was conducted on consecutive sections, and showed positive staining of both markers within the cellular structure (Figure 5 C, D). Antibodies specific for GFP expression identified the avian origin of the cell condensations (Figure 5 A).

Our previous studies demonstrated that human (HLA+) cells remain viable following *in vivo* culture on CAM (Moreno-Jiménez *et al.*, 2016). However, the current results indicated that RUNX2+/SOX9+ cell condensations co-localised with GFP expression, only present on the avian cells. To investigate the origin (human or avian) of the cells responsible for the formation of new bone, bone cylinders were decellularized (H_2O_2-treatment) or maintained in standard culture conditions (control) before CAM-implantation. No apparent differences in bone volume change were found between H_2O_2-

treated bone cylinders (6.84 % ± 3.7 SD) and standard culture conditions (control; 7.68 ± 3.38 SD; Figure 5 G). Histologically, control bone cylinders showed greater extracellular matrix deposition compared to H_2O_2-treatment (Figure 5 E-F), however no further clear differences between treatments were observed. Together, these results indicate that avian (GFP+) cells rather than human cells were responsible for the formation of SOX9+/RUNX2+ condensations and the concurrent increases in bone volume.

Evaluation of the osteoinductive properties of BMP2 in the CAM as a short term in vivo model

Previous results demonstrated that implantation of decellularized bone was sufficient to elicit comparable deposition of X-ray dense material as seen with living bone cylinders (Figure 5 G), suggesting that the endogenous growth factors entrapped within bone matrix (for example BMPs) may be responsible for the osteogenic response. To examine the ability of the CAM to respond as an *in vivo* model of ectopic bone, a commercial acellular collagen sponge (ACS) containing supra-physiological doses of BMP2 (2.4 µg BMP2) or vehicle control (0 µg BMP2) was implanted on the CAM for 9 days or cultured *in vitro* for the same period, followed by µCT and histological analysis. ACSs were integrated by the CAM as shown by the extensive deposition of collagen and proteoglycan tissue (Figure 6 A, A-1). In contrast, no tissue was formed on the *in vitro* ACS culture (compare Figure 6 B-1 and A-1).

After incubation, µCT analysis of the ACS showed a change in mineral deposition following BMP2 delivery (0.67 ± 0.56 SD mm^3; Figure 6 E) compared to vehicle control (0.44 ± 0.43 SD mm^3; Figure 6 E) on CAM-implanted samples, however this was not significant. There was negligible mineral deposition for the ACS cultured *in vitro* regardless of BMP2 delivery (0.0068 ± 0.006 SD mm^3; 0. 0012 ± 0.001 SD mm^3 respectively; Figure 6 E). In agreement with the µCT results, von Kossa staining showed mineral deposition (black pigmentation) on the CAM-implanted ACSs following BMP2 delivery (Figure 6 D, D-1), compared to the negligible presence of mineral in the vehicle control (Figure 6 C, D-1). Furthermore, mineral deposition was associated with cellular and matrix dense regions (see arrows Figure 6 D-1) and cell condensations (see asterisk Figure 6 D-1) with

similar appearance as previously shown with human bone cylinder implantation (Figure 5). These findings indicate BMP2 delivery on the CAM results in biomineralisation within the implanted scaffold and on the surrounding avian membrane.

Discussion

The aim of the present study was to understand and demonstrate the mechanisms of bone formation in a novel short-term *in vivo* model for tissue engineering: the CAM assay for the culture of living human bone. The current study has shown the ability of 3D registration of µCT scans to visualise the newly mineralised matrix on CAM-implanted human bone cylinders, followed by histology to validate the formation of new osteoid. Immunohistochemistry demonstrated the presence of markers of bone resorption (Cathepsin K) and osteoprogenitor cells (SOX9, RUNX2) on the CAM-implanted bone cylinders, co-localising with GFP staining (only expressed by the avian cells). Moreover, the increase in bone volume following *in vivo* implantation of bone cylinders was not dependent on the presence of human cells, indicating the role of endogenous growth factors from the bone matrix. Finally, CAM-implantation for 9 days of acellular ACSs loaded with an osteoinductive factor, BMP2, resulted in the formation of mineral deposits evidenced by von Kossa staining and µCT analysis.

In agreement with our previous study (Moreno-Jiménez *et al.*, 2016), we demonstrated that CAM-implantation of human viable bone cylinders resulted in a significant increase in bone volume (9.79 % ± 2.24 SD; $p<0.001$). The pre-existing mineralised tissue of the bone cylinder prevented the quantification or visualisation of the newly formed bone alone. To circumvent this limitation, 3D registration was used to align consecutive scans and subtract one from another, allowing the observation of negative (resorbed bone) and positive changes (formed bone) within the bone cylinders. Scans of control cylinders (where a non-treated bone cylinder was scanned sequentially prior to registration) showed that the process of 3D registration was not perfect, with a background of misaligned voxels and a small net change in bone volume (-0.3 %). This misalignment error is

commonly described in the literature, and shown to decrease with higher scanning resolution (Waarsing *et al.*, 2004; Schulte *et al.*, 2011; Birkhold *et al.*, 2014). Other authors scanning at similar resolutions to the present study (18 µm) have described this type of error upon 3D registration of control subjects, again associated with no changes in other architectural parameters such as bone volume (Waarsing *et al.*, 2004). To control for the misalignment error, bone cylinders were maintained at 4 ºC as internal control in each experiment. In marked contrast to the internal control and *in vitro* culture group, CAM-implanted bone cylinders showed a significant positive difference following 3D registration (Figure 2), with an 8.13 % increase in bone volume. Thus, despite the limitations of the analysis, 3D registration proved a successful method to visualise newly mineralised structures on CAM-implanted bone cylinders.

In agreement with the positive changes demonstrated by µCT analysis, new osteoid deposition was observed in the histology of trabecular bone from CAM-implanted bone cylinders. Given that bone cylinders were harvested from a living femoral head prior to *in vivo* implantation, it is possible that the on-going remodelling cycle of the bone tissue could have been maintained and/or stimulated upon implantation on the CAM, compared to *in vitro* cultured cylinders from the same patient. Previous studies showed fluorescent calcein deposition as early as four days post-fracture (Pautke *et al.*, 2005), similar to our implantation window of 9 days. Indeed, it is well known that the CAM is responsible for calcium transport from the egg-shell to the chick embryo to allow for skeleton mineralisation during an equivalent time-period (Tuan, 1980; Kanczler *et al.*, 2012). In addition to osteoid deposition, a marker of bone resorption (Cathepsin K) was observed on CAM-implanted bone cylinders, and co-localised with GFP expression from the avian cells. The osteoclastic/bone resorptive ability of the CAM was documented as early as 1990 when Webber *et al.* implanted decellularised bovine bone fragments on the CAM and showed significant resorption pits on acellular bone chips following implantation (Webber, Menton and Osdoby, 1990). Thus, the observation of osteoclast activity on the CAM-implanted bone cylinders was to be expected, in particular given that; i) certain regions of the bone cylinders may be necrotic due to a lack of oxygen and nutrient supply during the harvest procedure, hence requiring osteoclast-mediated removal and, ii) the invasion of avian blood vessels

within the bone cylinder, critical for the influx of osteoclast precursors (Udagawa *et al.*, 1990). Overall, these results support the conclusion that the CAM assay provides a vascular component in which bone tissue formation and resorption (thus bone remodelling) can be evaluated *in vivo* short-term. Crucially, these studies show the utility of the CAM system in modelling human bone physiology *ex vivo*, as well as demonstrating the role of osteogenic factors within a living human bone tissue-avian hybrid model.

In addition to bone remodelling, evidence of preliminary ectopic ossification was observed within the CAM. Cell condensations strongly expressing SOX9 and RUNX2 proteins, essential transcription factors for endochondral bone formation (Akiyama *et al.*, 2002), were observed in the CAM tissue in proximity to the human bone cylinder. These cell condensations also co-stained with GFP, confirming their avian origin. We formerly described the formation of these cell condensations in association with collagen type II deposition from the CAM, again co-expressing with SOX9 and GFP next to the human bone tissue (Moreno-Jiménez *et al.*, 2016). Early studies from Hancox showed formation of similar cell condensations following engraftment of chick embryo calvaria fragments on CAM (Hancox, 1946). Other authors have implanted agarose/gelatine beads carrying BMP7 and shown the formation of comparable clusters of cells as well as significant stratification of the CAM extracellular matrix (Ramoshebi and Ripamonti, 2000). In agreement with this, we also observed the formation of cellular condensations within the CAM following implantation of ACS containing BMP2 for 9 days (Figure 6). Furthermore, von Kossa staining on non-decalcified sections showed the presence of mineral deposition within the condensations in the ACS-BMP2 group, but absent in the vehicle control group (Figure 6). Additional studies in the literature have cultured placenta-derived multipotent stem cells *in vitro* and showed their differentiation potential towards osteogenic, chondrogenic and adipogenic lineages, demonstrating the plasticity of cells derived from an extraembryonic membrane (Miki *et al.*, 2005; Ulrich *et al.*, 2013). Thus, the formation of endochondral cell condensations (SOX9+, RUNX2+) and mineral deposition within the CAM indicate the ability of the CAM to respond to an osteoinductive stimuli.

In our previous study, we demonstrated the presence of human viable cells following CAM-implantation and *in vitro* culture of human bone cylinders (Moreno-Jiménez *et al.*, 2016). Given that evidence of new bone (increase in bone volume, osteoid deposition and formation of cell condensations) was only present in CAM-implanted bone cylinders, and that that expression of bone formation markers (SOX9, RUNX2) appeared to be of avian origin (GFP+), we questioned the role of human cells in this process, despite their survival following CAM-implantation (Moreno-Jiménez *et al.*, 2016). Decellularised human bone cylinders (H_2O_2-treated) showed a similar increase in bone volume following *in vivo* implantation compared to viable bone cylinders, hence excluding the human cells as the main source of the observed active mineral deposition. This was not a surprising finding considering: i) endogenous growth factors within bone matrix such as BMPs and IGFs are known to have osteoinductive potential (Urist and Daly, 1965; Hayden, Mohan and Baylink, 1995), ii) allograft bone remains a standard source of bone graft material for clinical use and iii) the vigorous growth of embryo-derived cells (avian) compared to elderly patient cells (human). To evaluate whether BMP2 alone was sufficient to induce bone formation, ACS containing BMP2 were CAM-implanted for 9 days. However, no significant difference in mineral deposition was observed with respect to vehicle control (0.67 ± 0.56 SD mm^3 vs 0.437 ± 0.43 SD mm^3). However, in comparison with other models of ectopic bone formation, the dose utilised within these CAM studies (2.4 µg BMP2) was significantly lower in contrast to other species such as the mouse or rat (115.3 - 150 µg BMP2) (Wang *et al.*, 1990; Luca *et al.*, 2011; Cai *et al.*, 2014). In addition, the implantation period was significantly shorter (9 days) compared to the standard 4-6 weeks in murine hosts (Wang *et al.*, 1990; Luca *et al.*, 2011; Cai *et al.*, 2014). Nevertheless, von Kossa staining showed a marked difference between BMP2 and vehicle control in terms of mineral deposition, evidence of the early stages of the ectopic ossification process within the CAM, and hence potentially resulting in greater differences if the incubation period could be extended.

While the CAM assay has shown its utility for bone remodelling of human tissue *ex vivo* (Figure 3-4), this short-term implantation model cannot substitute already established *in vivo* models important in the examination of biomaterials in the context of physiological processes, such as a full immune response and mechanical load. Nevertheless, the CAM assay offers a simple, cost-effective and minimally invasive short-term *in vivo* model, which can serve as a promising high-throughput screening platform for the study of early stages of bone formation, angiogenesis and biocompatibility. Finally, considering the limited number of publications exploiting the CAM assay in the field of tissue engineering and biomaterial testing, these current studies demonstrate the osteogenic potential of the CAM to serve as a critical stepping-stone between *in vitro* and future *in vivo* studies, allowing for refinement and reduction in the use of animal experiments in later stages of the preclinical research.

Conclusion

In summary, the current study supports the concept that ossification is occurring within viable human bone cylinders implanted on the CAM. We demonstrate that, despite the pre-existing mineralised matrix in the bone cylinders, μCT image analysis (3D registration) can be used to visualise and quantify the newly mineralised matrix following CAM-implantation. Histological analysis demonstrated that the changes in bone volume were due to i) an on-going bone remodelling process from the pre-existing trabecular bone, evidenced by new osteoid deposition and expression of osteoclast markers (Cathepsin K) and, ii) deposition of new mineralised matrix, possibly through CAM-derived ectopic bone formation (SOX9 and RUNX2 cell condensations). Finally, the current study establishes that avian cells, and not human cells, were responsible for the matrix mineralisation observed and the avian cells could thus respond to osteoinductive stimuli. The present findings offer further insights into the mechanics of a novel, short-term, humanised *in vivo* model for the screening of novel therapies and biomaterials with considerable implications therein for tissue engineering and regenerative medicine.

Materials and Methods

Bone cylinders preparation

Bone cylinders were harvested from adult femoral heads collected from haematologically normal patients (aged 67-85) undergoing routine elective hip replacement surgery. Four osteoarthritic donors (three males aged 49, 79 and 68, and one female aged 67) and three osteoporotic donors (one male aged 79 and two females aged 81 and 85). Only one patient (F85 NOF) out of seven was found to be significantly different with respect to the others (see Supplementary Figure 4). Only tissue that would have been discarded from surgery was used following informed consent from the patients in accordance with approval from Southampton & South West Hampshire Local Research Ethics Committee (Ref: 194/99/w) (see (Moreno-Jiménez *et al.*, 2016)).

Harvested bone cylinders (6 mm outer diameter, 2 mm empty core and 4-6 mm in length) were prepared for *in vitro* culture (organotypic), CAM-implantation or maintained at 4˚C as control. Organotypic or transwell cultures were conducted in serum-free basal media at 37 ˚C and 5% CO_2 for 9 days and media was replaced every other day as detailed in (Moreno-Jiménez *et al.*, 2016). A minimum of 8-10 samples per group for CAM assay (*in vivo*) and a minimum of 5-6 samples for *in vitro* groups were included in each independent experiment.

Decellularisation of bone cylinders

To destroy endogenous cells in the bone tissue, the bone cylinders were submerged in 30 % hydrogen peroxide with repeated changes for 3 days and maintained at 4˚C. Thereafter, decellularised bone cylinders (n=8-10) were thoroughly washed three times in sterile PBS for 2 hours with rotation, before resuming the CAM protocol.

Acellular collagen sponges (ACS) – BMP2

Lyophilised rhBMP2 (dibotermin alfa, InductOs™, Medtronics, USA) was reconstituted to give a concentration of 1500 µg/ml BMP2. A working concentration (150 µg/ml) solution was prepared in formulation buffer (2.5% glycine, 0.5% sucrose, 0.01% Polysorbate 80, 5 mM sodium chloride and 5 mM L-glutamic acid, pH 4.5), in low-protein binding Eppendorf tubes at 4 °C to preserve bioactivity

one hour before application. Standard sized acellular collagen sponges (ACS) were impregnated with 16 µl of the BMP2 working solutions (2.4 µg BMP2) or with solution buffer (vehicle control with 0 µg BMP2) and incubated for 10 minutes before implantation on the CAM or *in vitro* culture for 9 days. *In vitro* culture was conducted in transwells with serum-free basal media, maintained in 5 % CO_2 at 37 ˚C, and media replaced every other day. A minimum of 8-10 samples per group for CAM assay and a minimum of 5-6 samples for *in vitro* groups were included in each independent experiment.

CAM assay

Genetically modified chick embryos expressing green fluorescent protein (GFP) were kindly donated by Dr Adrian Sherman from the Transgenic Chicken Facility at the Roslin Institute (Edinburgh, UK) (McGrew *et al.*, 2004). The eggs were incubated for 9-10 days at 37 ˚C in a 60 % humidified atmosphere with rotation programmed every hour in a Hatchmaster incubator. At day 9-10 of incubation, an approximately 1 cm^2 window was cut in the eggshell, and the implant was carefully placed on the CAM (Figure 1). Please see reference for more information about the CAM assay protocol (Moreno-Jimenez *et al.*, 2017; Moreno-Jiménez *et al.*, 2017). Sterile parafilm was used to seal the eggshell window and the eggs incubated for another 9 days without rotation . Embryos were monitored daily and the number of fully developed chick embryos, according to Hamburger and Hamilton (V. Hamburger, 1951), was recorded when the gestational process was terminated. All animal procedures were carried out in accordance with the guidelines and regulations laid down in the Animals (Scientific Procedures) Act 1986. Chick embryo CAM model was carried out according to Home Office Approval, UK (Project license – PPL 30/2762).

Micro computed tomography (µCT) analysis

Bone cylinders were scanned before and after incubation using the same parameters. The cylinders were scanned in plastic Eppendorf tubes using a high resolution computed tomography SkyScan 1176 scanner and analysed using Dataviewer (version 1.5.2.4) and CTAn software (version 1.16) software (Bruker, Kontich, Belgium). Scans were conducted using the following settings: X-ray source 50 kV, 500 µA, rotation step 0.55°, exposure time 496 ms, averaging (1) and an average voxel size of 18 µm.

The estimated radiation dose for the scan conditions was 100 mGy. Raw data were reconstructed using NRcon software with correction for misalignment, ring artefacts (6), smoothing (3) and beam hardening (30%). A global threshold was applied to pre- and post- binary datasets and CTan software analysis provided the bone volume. Bone volume change was calculated as post with respect to pre scan of individual bone cylinders.

Collagen sponge scans were conducted using the following settings: X-ray source 40 kV, 600 µA, exposure time 496 ms, averaging of 3, rotation step 0.5° and an average voxel size of 18 µm. The raw data were reconstructed and analysed as described above to quantify bone volume (mm^3).

Histology and immunohistochemistry analysis

Bone cylinders were fixed in 4% paraformaldehyde in 1x PBS at 4 ˚C for 24 hours and acid-decalcified by incubating in Histoline (Histoline, Milan, Italy) for 24 hours with rotation at 4 ˚C. Samples were then processed for paraffin sectioning (5 µm) and stained as described by Kanczler *et al* (Kanczler *et al.*, 2012) for Alcian Blue (proteoglycans) and Sirius Red (collagen). Immunohistochemistry for SOX9 (AB5535), RUNX2 (ab23981), GFP (2555) and Cathepsin K (ab66237) was performed as described by Kanczler *et al*. (Kanczler *et al.*, 2012). For specific details of antigen retrieval and antibody concentrations, see Supplementary Table 1. Please note that boiling of the sections may result in loss of adherence to the slide. Positive immunostaining was shown as brown/red, matrix was counterstained with Alcian Blue (proteoglycans) and IgG isotype antibody was used for controls. Acelluar collagen sponges were processed as described above omitting the decalcification step, von Kossa staining was performed as described by Kanczler *et al*. (Kanczler *et al.*, 2012). Mineralised tissue processing in resin, sectioning and Goldner's Trichrome staining of bone cylinders was kindly conducted at the skelet.AL Skeletal Analysis Laboratories, University of Sheffield, UK. Images were captured with an Olympus BX-51/22 dotSlide digital virtual microscope.

Statistical analysis

All experimental data was analysed using Statistical Analysis SPSS Base 16.0 software for Windows. Results were expressed as the mean ± SD and plotted using GraphPad Prism. Data distribution was examined using Kolmogorov-Smirnov test to determine normality. A minimum of 8-10 samples per group for CAM assay and a minimum of 5-6 samples for *in vitro* groups were included in each independent experiment. Only data from viable chick-eggs and CAM-integrated samples (bone cylinders, ACS) were included for analysis. Comparisons between two treatments were performed using student t-test. Comparisons between more than 2 treatments were performed using the one-way ANOVA test including Tukey post-hoc test. Values of $p<0.05$ were considered statistically significant.

Acknowledgements

This study was supported by the National Centre for the Replacement, Reduction and Refinement of Animals in Research (NC3Rs; grant number NC/K500380/1) and by the European Union Seventh Framework Programme under grant agreement n° [318553]—SkelGEN and Programme Grant, BioDesign (262948). The authors would like to express their gratitude to Julia Wells for their technical support, Dr Jeroen Hostens and Dr Phil Salmon from Bruker MicroCT, Belgium, for their advice in μCT analysis, Dr Adrian Sherman for kindly providing the GFP-eggs for the experiments, and Dr Edoardo Scarpa and Dr Juan A. Nunez for their constructive comments on the manuscript.

Additional information

Competing financial interests: The authors declare no competing financial interests.

Author contributions

Study design: IMJ, JMK, NDE and ROCO; Experimental work: IMJ; Data analysis and interpretation: IMJ, JMK, NDE and ROCO; Drafting manuscript: IMJ; Revising manuscript content: IMJ, JMK,

GHB, SAL, NDE and ROCO. Approving final version of manuscript: IMJ, JMK, GHB, SAL, NDE and ROCO. ROCO takes responsibility for the integrity of the data analysis.

Funding

This study was supported by the National Centre for the Replacement, Reduction and Refinement of Animals in Research (NC/K500380/1 NC3Rs) and by the European Union Seventh Framework Programme under grant agreement n° [318553]—SkelGEN and Programme Grant, BioDesign (262948).

References

Akiyama, H. *et al.* (2002) 'The transcription factor Sox9 has essential roles in successive steps of the chondrocyte differentiation pathway and is required for expression of Sox5 and Sox6', *Genes & Development*, 16, pp. 2813–2828. doi: 10.1101/gad.1017802.

Baiguera, S., Macchiarini, P. and Ribatti, D. (2012) 'Chorioallantoic membrane for in vivo investigation of tissue-engineered construct biocompatibility', *Journal of Biomedical Materials Research - Part B Applied Biomaterials*, 100 B(5), pp. 1425–1434. doi: 10.1002/jbm.b.32653.

Birkhold, A. I. *et al.* (2014) 'Mineralizing surface is the main target of mechanical stimulation independent of age: 3D dynamic in vivo morphometry', *Bone*. Elsevier Inc., 66, pp. 15–25. doi: 10.1016/j.bone.2014.05.013.

Cai, W. X. *et al.* (2014) 'Effect of different rhBMP-2 and TG-VEGF ratios on the formation of heterotopic bone and neovessels', *BioMed Research International*, 2014, pp. 1–7. doi: 10.1155/2014/571510.

Carre, A. L. *et al.* (2012) 'Fetal Mouse Skin Heals Scarlessly in a Chick Chorioallantoic Membrane Model System', *Annals of Plastic Surgery*, 69(1), pp. 85–90. doi: 10.1097/SAP.0b013e31822128a9.

Coconi, M. T. *et al.* (2005) 'Angiogenic response induced by acellular aorta matrix in vivo', *Journal of Anatomy*, 207(1), pp. 79–83. doi: 10.1111/j.1469-7580.2005.00427.x.

Collin-Osdoby, P. *et al.* (2000) 'Decreased Nitric Oxide Levels Stimulate Osteoclastogenesis and Bone Resorption Both in Vitro and in Vivo on the Chick Chorioallantoic Membrane in Association with Neoangiogenesis', *Journal of Bone and Mineral Research*, 15(3), pp. 474–488. doi: 10.1359/jbmr.2000.15.3.474.

V. Hamburger, H. L. H. (1951) 'A series of normal stages in the development of the chick embryo', *Journal of Morphology*, 88(1), pp. 49–92. doi: 10.1002/aja.1001950404.

Hancox, N. M. (1946) 'The survival of transplanted embryo bone grafted to CAM and subsequent

osteogenesis', *Journal of physiology*, 106(1923), pp. 279–285. doi: 10.1113/jphysiol.1947.sp004211.

Hayden, J. M., Mohan, S. and Baylink, D. J. (1995) 'The insulin-like growth factor system and the coupling of formation to resorption.', *Bone*, 17(2 Suppl), p. 93S–98S. Available at: http://www.ncbi.nlm.nih.gov/pubmed/8579905

Holzapfel, B. M. *et al.* (2015) 'Tissue engineered humanized bone supports human hematopoiesis in vivo', *Biomaterials*, 61, pp. 103–114. doi: 10.1016/j.biomaterials.2015.04.057.

Ito, R. *et al.* (2012) 'Current advances in humanized mouse models.', *Cellular & molecular immunology*, 9(3), pp. 208–14. doi: 10.1038/cmi.2012.2.

Kanczler, J. M. *et al.* (2007) 'Supercritical carbon dioxide generated vascular endothelial growth factor encapsulated poly(dl-lactic acid) scaffolds induce angiogenesis in vitro', *Biochemical and Biophysical Research Communications*, 352(1), pp. 135–141. doi: 10.1016/j.bbrc.2006.10.187.

Kanczler, J. M. *et al.* (2012) 'A novel approach for studying the temporal modulation of embryonic skeletal development using organotypic bone cultures and microcomputed tomography.', *Tissue engineering. Part C, Methods*, 18(10), pp. 747–60. doi: 10.1089/ten.TEC.2012.0033.

Kanczler, J. M. and Oreffo, R. O. C. (2008) 'Osteogenesis and angiogenesis: The potential for engineering bone', *European Cells and Materials*. SWISS SOC BIOMATERIALS, 15, pp. 100–114. doi: vol015a08 [pii].

Keshaw, H. *et al.* (2010) 'Microporous collagen spheres produced via thermally induced phase separation for tissue regeneration', *Acta Biomaterialia*. Acta Materialia Inc., 6(3), pp. 1158–1166. doi: 10.1016/j.actbio.2009.08.044.

Kilarski, W. W. *et al.* (2012) 'An in vivo neovascularization assay for screening regulators of angiogenesis and assessing their effects on pre-existing vessels', *Angiogenesis*, 15(4), pp. 643–655. doi: 10.1007/s10456-012-9287-8.

Kunzi-Rapp, K., Rück, A. and Kaufmann, R. (1999) 'Characterization of the chick chorioallantoic membrane model as a short-term in vivo system for human skin.', *Archives of dermatological research*, 291(5), pp. 290–5.

Lee, M. K. *et al.* (2015) 'A bio-inspired, microchanneled hydrogel with controlled spacing of cell adhesion ligands regulates 3D spatial organization of cells andtissue', *Biomaterials*. Elsevier Ltd, 58, pp. 26–34. doi: 10.1016/j.biomaterials.2015.04.014.

Lokman, N. a. *et al.* (2012) 'Chick chorioallantoic membrane (CAM) assay as an in vivo model to study the effect of newly identified molecules on ovarian cancer invasion and metastasis', *International Journal of Molecular Sciences*, 13(8), pp. 9959–9970. doi: 10.3390/ijms13089959.

Luca, L. *et al.* (2011) 'Injectable rhBMP-2-loaded chitosan hydrogel composite: Osteoinduction at ectopic site and in segmental long bone defect', *Journal of Biomedical Materials Research - Part A*, 96 A(1), pp. 66–74. doi: 10.1002/jbm.a.32957.

Maeda, Y. and Noda, M. (2003) 'Coordinated development of embryonic long bone on chorioallantoic membrane in ovo prevents perichondrium-derived suppressive signals against cartilage growth', *Bone*, 32(1), pp. 27–34. doi: 10.1016/S8756-3282(02)00917-1.

Martinez-Madrid, B. *et al.* (2009) 'Chick embryo chorioallantoic membrane (CAM) model: a useful tool to study short-term transplantation of cryopreserved human ovarian tissue.', *Fertility and sterility*, 91(1), pp. 285–92. doi: 10.1016/j.fertnstert.2007.11.026.

McGrew, M. J. *et al.* (2004) 'Efficient production of germline transgenic chickens using lentiviral vectors.', *EMBO reports*, 5(7), pp. 728–33. doi: 10.1038/sj.embor.7400171.

Miki, T. *et al.* (2005) 'Stem cell characteristics of amniotic epithelial cells.', *Stem cells (Dayton, Ohio)*, 23(10), pp. 1549–59. doi: 10.1634/stemcells.2004-0357.

Moreno-Jimenez, I. *et al.* (2017) 'The chorioallantoic membrane (CAM) assay for biomaterial testing in tissue engineering: a short term in vivo preclinical model', *Tissue Engineering Part C: Methods*, 0(0), p. ten.TEC.2017.0186. doi: 10.1089/ten.TEC.2017.0186.

Moreno-Jiménez, I. *et al.* (2016) 'The chorioallantoic membrane (CAM) assay for the study of human bone regeneration: a refinement animal model for tissue engineering', *Scientific Reports*. Nature Publishing Group, 6(April), p. 32168. doi: 10.1038/srep32168.

Moreno-Jiménez, I. *et al.* (2017) 'The chorioallantoic membrane (CAM) assay for biomaterial testing in tissue engineering: a short term in vivo preclinical model', *Tissue Engineering, Part C: Methods*. NIH Public Access.

Murphy, J. B. (1913) 'TRANSPLANTABILITY OF TISSUES TO THE EMBRYO OF FOREIGN SPECIES: ITS BEARING ON QUESTIONS OF TISSUE SPECIFICITY AND TUMOR IMMUNITY.', *Journal of Experimental Medicine*. Rockefeller University Press, 17(4), pp. 482–493. doi: 10.1084/jem.17.4.482.

Nowak-Sliwinska, P., Segura, T. and Iruela-Arispe, M. L. (2014) 'The chicken chorioallantoic membrane model in biology, medicine and bioengineering', *Angiogenesis*, 17(4), pp. 779–804. doi: 10.1007/s10456-014-9440-7.

Pautke, C. *et al.* (2005) 'Polychrome labeling of bone with seven different fluorochromes: Enhancing fluorochrome discrimination by spectral image analysis', *Bone*, 37(4), pp. 441–445. doi: 10.1016/j.bone.2005.05.008.

Ramoshebi, L. N. and Ripamonti, U. (2000) 'Osteogenic protein-1, a bone morphogenetic protein, induces angiogenesis in the chick chorioallantoic membrane and synergizes with basic fibroblast growth factor and transforming growth factor-beta1.', *The Anatomical record*, 259(1), pp. 97–107.

Ribatti, D. *et al.* (2003) 'Angiogenic response induced by acellular brain scaffolds grafted onto the chick embryo chorioallantoic membrane', *Brain Research*, 989(1), pp. 9–15. doi: 10.1016/S0006-8993(03)03225-6.

Ribatti, D. *et al.* (2006) 'The gelatin sponge-chorioallantoic membrane assay.', *Nature protocols*, 1(1), pp. 85–91. doi: 10.1038/nprot.2006.13.

Rous, P. and Murphy, J. (1911) 'Tumor implantation in the developing embryo', in *Journal of the American Medical Association*. American Philosophical Society, p. 740. doi: 10.1001/jama.1911.02560100032014.

Russel, W. M. S and Burch, R. . (1959) *The Principles of Humane Experimental Technique*. 18th edn. London, Methuen: Harvard.

Schulte, F. A. *et al.* (2011) 'In vivo micro-computed tomography allows direct three-dimensional quantification of both bone formation and bone resorption parameters using time-lapsed imaging', *Bone*. Elsevier Inc., 48(3), pp. 433–442. doi: 10.1016/j.bone.2010.10.007.

Smith, E. L., Kanczler, J. M. and Oreffo, R. O. C. (2013) 'A new take on an old story: Chick limb organ culture for skeletal niche development and regenerative medicine evaluation', *European Cells and Materials*, 26, pp. 91–106.

Stallmach, T. *et al.* (2001) 'Feto-maternal interface of human placenta inhibits angiogenesis in the chick chorioallantoic membrane (CAM) assay', *Angiogenesis*, 4(1), pp. 79–84. doi: 10.1023/A:1016769416713.

Takahashi, K. *et al.* (1991) 'Fracture healing of chick femurs in tissue culture.', *Acta orthopaedica Scandinavica*, 62(4), pp. 352–5.

Tuan, R. S. (1980) 'Calcium transport and related functions in the chorioallantoic membrane of cultured shell-less chick embryos', *Developmental Biology*. Academic Press, 74(1), pp. 196–204. doi:

10.1016/0012-1606(80)90061-5.

Udagawa, N. *et al.* (1990) 'Origin of osteoclasts: mature monocytes and macrophages are capable of differentiating into osteoclasts under a suitable microenvironment prepared by bone marrow-derived stromal cells.', *Proceedings of the National Academy of Sciences of the United States of America*, 87(18), pp. 7260–7264. doi: 10.1073/pnas.87.18.7260.

Ulrich, C. *et al.* (2013) 'Low osteogenic differentiation potential of placenta-derived mesenchymal stromal cells correlates with low expression of the transcription factors Runx2 and Twist2.', *Stem cells and development*, 22(21), pp. 1–38. doi: 10.1089/scd.2012.0693.

Urist, M. R. and Daly, J. (1965) 'Bone: formation by autoinduction', *Science*, 150(698), pp. 893–899. doi: 11937861.

Waarsing, J. H. *et al.* (2004) 'Detecting and tracking local changes in the tibiae of individual rats: A novel method to analyse longitudinal in vivo micro-CT data', *Bone*, 34(1), pp. 163–169. doi: 10.1016/j.bone.2003.08.012.

Wang, E. a *et al.* (1990) 'Recombinant human bone morphogenetic protein induces bone formation.', *Proceedings of the National Academy of Sciences of the United States of America*, 87(6), pp. 2220–2224. doi: 10.1073/pnas.87.6.2220.

Webber, D. M., Menton, D. and Osdoby, P. (1990) 'An in vivo model system for the study of avian osteoclast recruitment and activity', *Bone and Mineral*, 11, pp. 127–140.

Xiao, X. *et al.* (2015) 'Chick chorioallantoic membrane assay: A 3D animal model for study of human nasopharyngeal carcinoma', *PLoS ONE*, 10(6), pp. 1–13. doi: 10.1371/journal.pone.0130935.

Yang, X. B. *et al.* (2004) 'Human osteoprogenitor bone formation using encapsulated bone morphogenetic protein 2 in porous polymer scaffolds', *Tissue engineering*, 10(7), pp. 1037–1047. doi: 10.1089/ten.2004.10.1037.

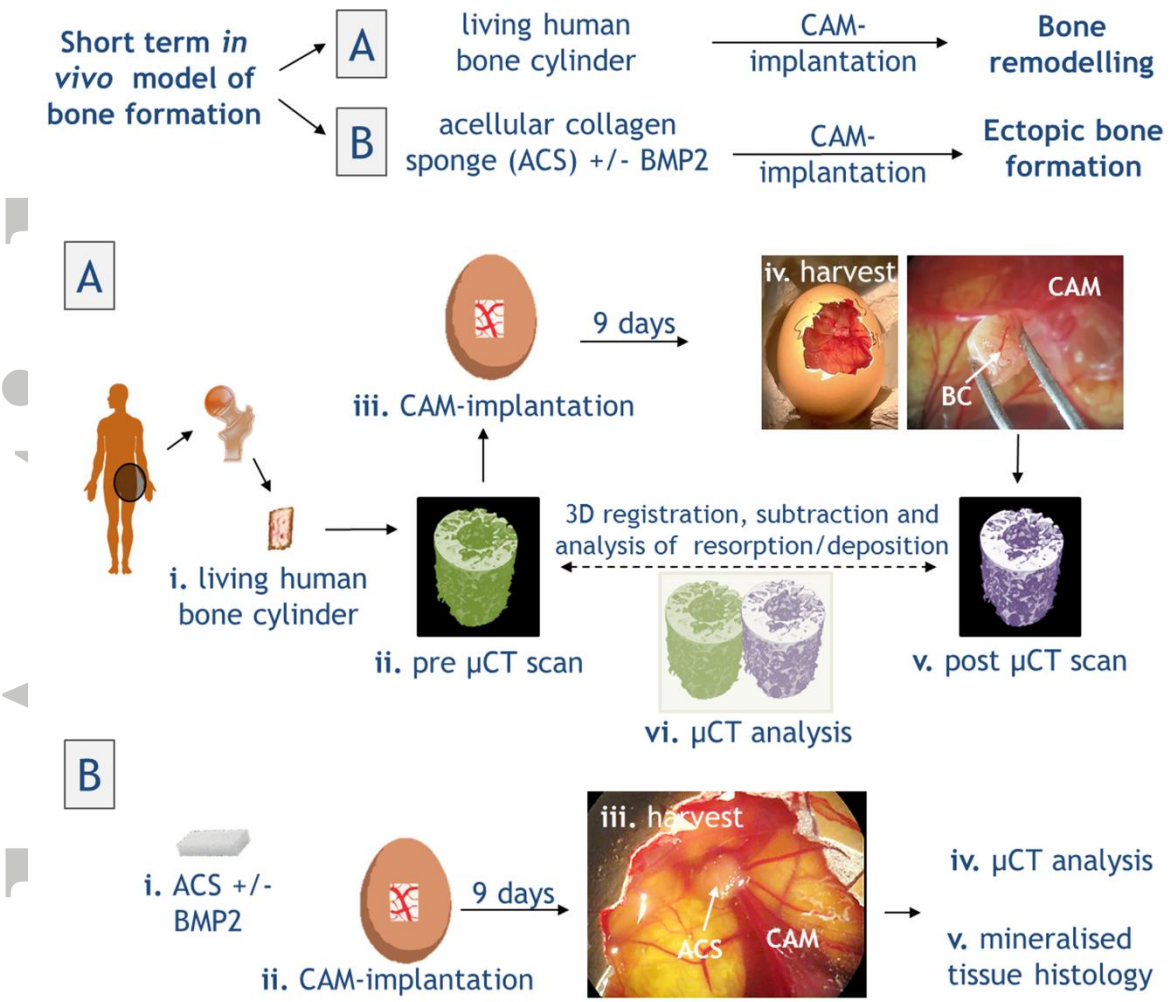

Figure 1: Pictorial illustration of the experimental design of the study. A. Human femoral heads were collected following surgery after informed patient consent. Bone cylinders (6 mm diameter, 5-6 mm length) were harvested from the femoral heads using a dentist surgical drill devised to contain a concentric empty-core of 2 mm (i). Bone cylinders (n=6-8 per group) were µCT-scanned (pre scan) individually (ii) prior to CAM-implantation for 9 days (iii), or alternatively cultured *in vitro* for the same period. At harvest (iv), bone cylinders were again µCT scanned (post scan) individually. Analyses of µCT included vi) quantification of the relative change in bone volume of the post scan with respect to the pre scan of individual bone cylinders and vi) 3D registration of pre and post scan for visualisation of the changes. **B.** Commercial acellular collagen sponges (ACS) of bovine origin containing ± 2.4 µg BMP2 (i) were implanted on the CAM for 9 days (ii). At harvest (iii) ACS were µCT scanned (iv) and processed for mineralised tissue histology (v). Only data collected from viable chick embryos and integrated graft samples was included for analysis. Chorioallantoic membrane (CAM), bone cylinder (BC), acellular collagen sponge (ACS).

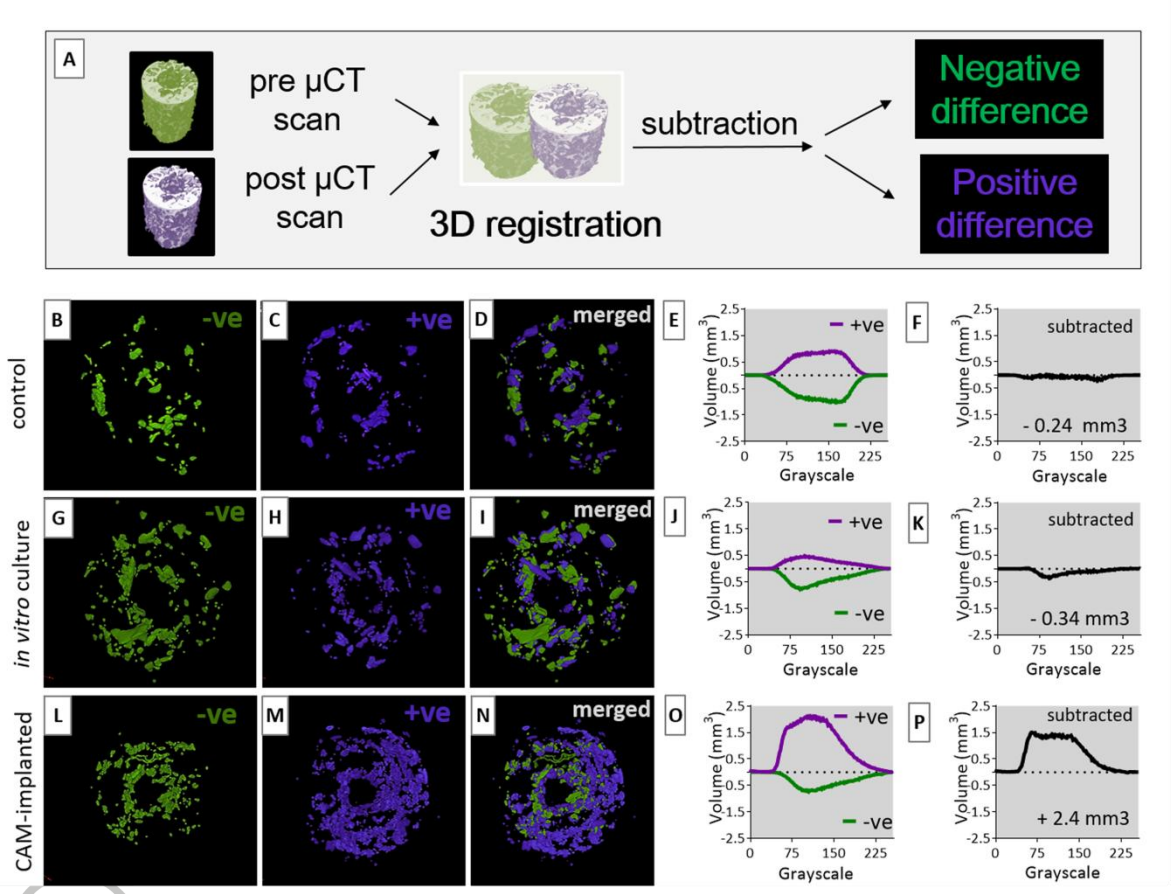

Figure 2: 3D Visualisation of new bone formation on human bone cylinders following CAM-implantation. A. 3D registration was used to align pre and post scans of individual human bone cylinders. Following registration**,** pre and post scans were subtracted one from another to allow visualisation of the negative (green) and positive (purple) difference, identifying voxels from the pre and post scan, respectively. **B-P.** Representative images of pre and post scans of bone cylinders under different culture conditions (CAM-implantation L-P, *in vitro* G-K or maintained at 4°C for internal control; B-F). Pre and post scans were superposed by 3D registration and subtracted to display negative difference in green (resorbed bone; B, G, L), positive difference in purple (newly formed bone; C, H, M), and merged (D, I, N). Constant structures were omitted to facilitate visualisation of the difference. The histogram in greyscale values (0-255) of the positive and negative difference were plotted (E, J, O) and subtracted one from another (F, K, P).

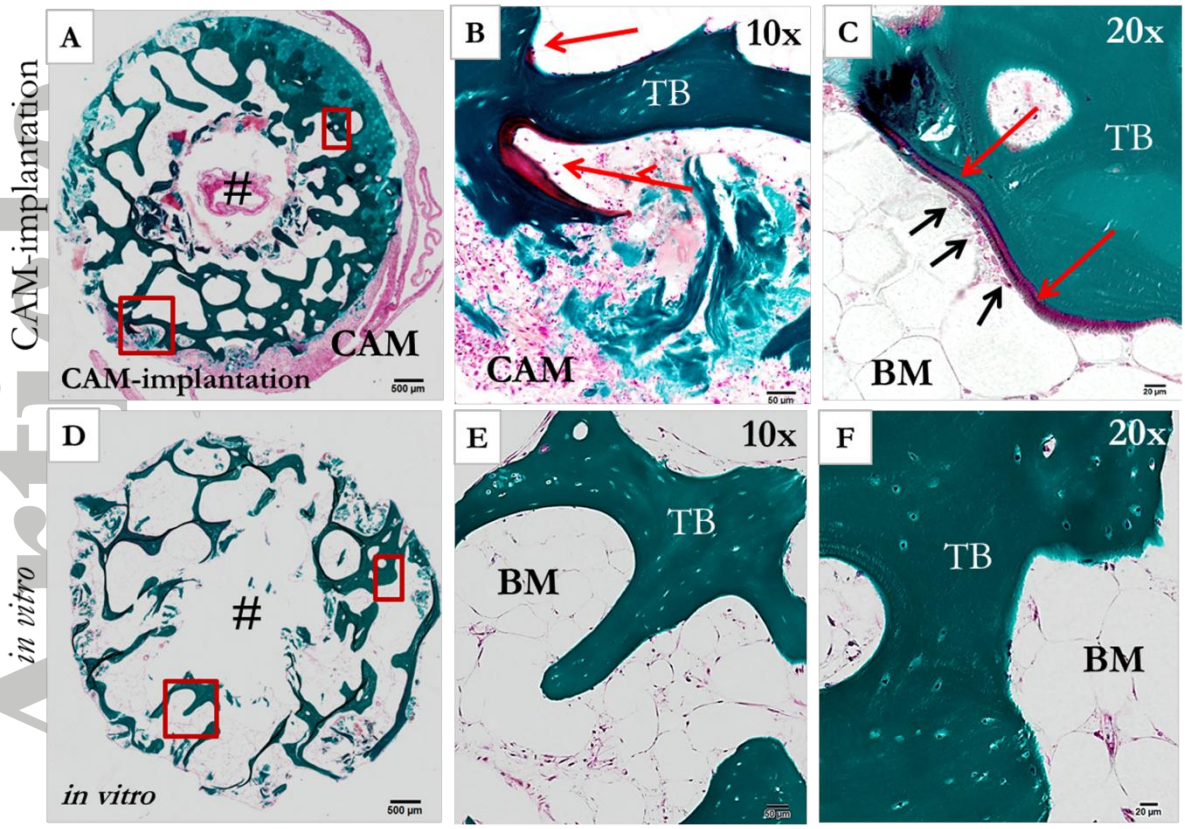

Figure 3: New osteoid deposition on human living bone cylinders following *in vivo* CAM-implantation. Bone cylinders were harvested from a femoral head immediately after patient surgery with a concentric defect created (#) before CAM-implantation (A-C) or *in vitro* culture (D-F) for 9 days. After incubation, bone cylinders were processed without decalcification. Representative images of Goldner's Trichrome staining: mineralised tissue (green), osteoid (dark red). Red arrows indicate osteoid deposition. Black arrows indicate osteoblast-like cells. # indicates bone defect area. Chorioallantoic membrane (CAM), trabecular bone (TB). Scale bars detailed equivalent to 500 µm (A, D), 50 µm (B, E) and 20 µm (C,F).

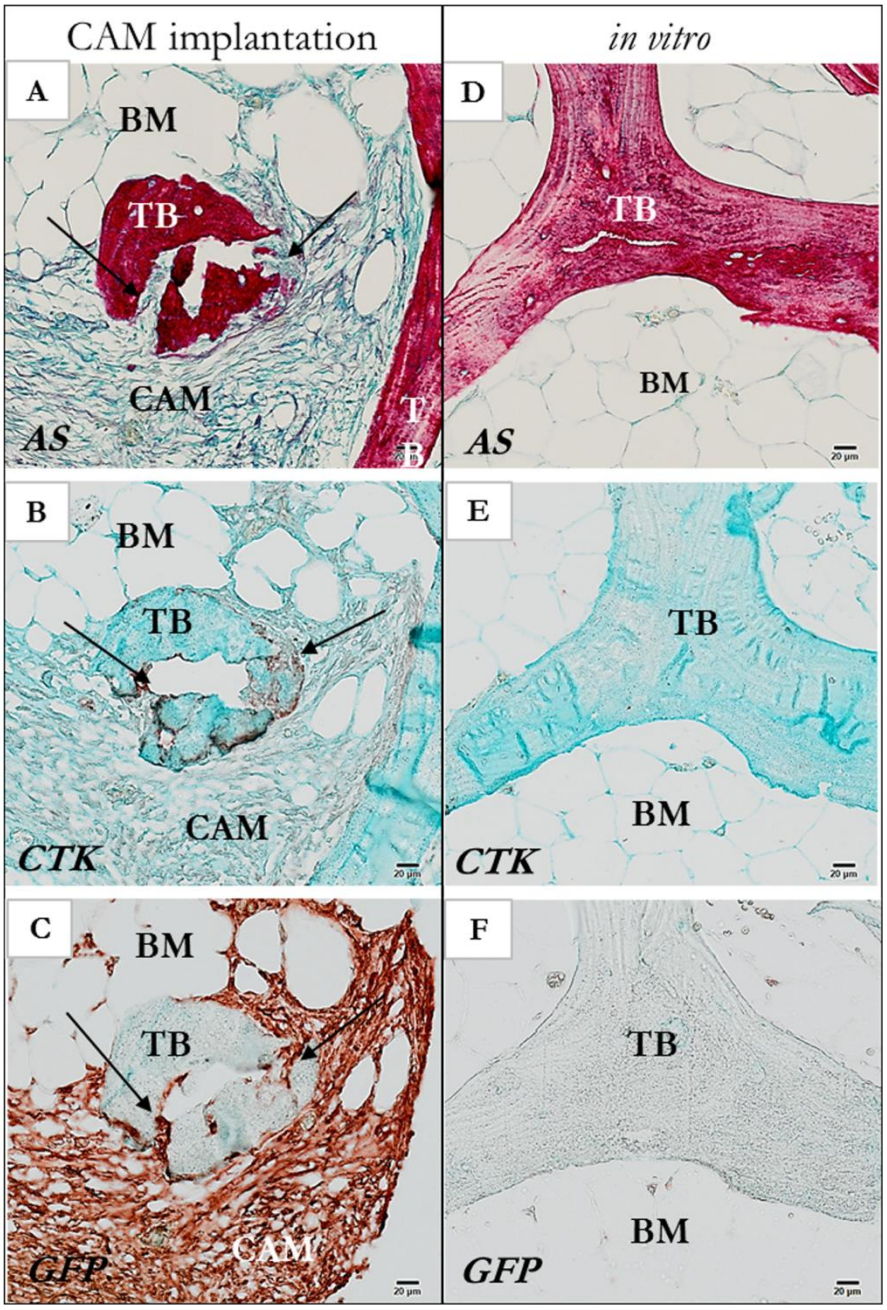

Figure 4: Osteoclast activity of avian origin present on human living bone cylinders following *in vivo* CAM-implantation. Bone cylinders were acid-decalcified and prepared for paraffin histology after CAM-implantation (A-C) or *in vitro* culture (D-F). Representative images of consecutive sections stained for Alcian Blue (proteoglycans) and Sirius Red (collagen) (A, D), immunohistochemistry to detect Cathepsin K (B, E) and green fluorescent protein (GFP) to identify avian tissue (C,F). Positive immunostaining in brown-red colour, counterstained with Alcian Blue to visualize the matrix content. Arrows indicate regions of co-localisation of GFP and CTK positive staining. # indicates bone defect area. Chorioallantoic membrane (CAM), trabecular bone (TB), AS (Alcian Blue and Sirius Red), CTK (Cathepsin K). Scale bars equivalent to 20 µm.

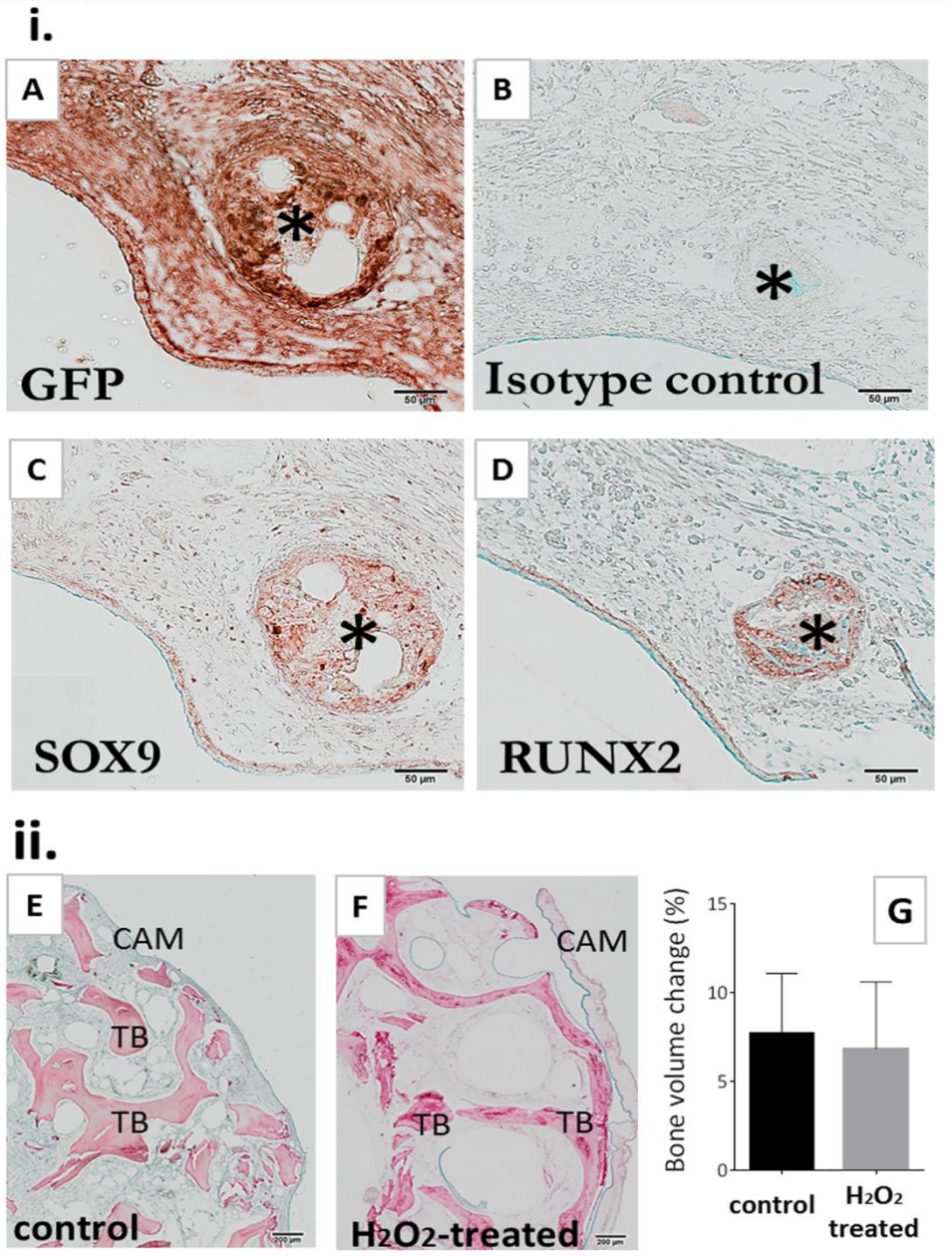

Figure 5: Avian-derived cells drive the increase in bone volume on CAM-implanted human bone cylinders and form RUNX2/SOX9 cell condensations. i. Bone cylinders implanted on GFP-CAM, harvested and processed for paraffin histology. Representative images of consecutive sections stained for immunohistochemistry to detect green fluorescent protein (A), SOX9 chondrogenic transcription factor (C) and RUNX2 osteogenic transcription factor (D). Positive immunostaining in brown-red colour, counterstained with Alcian Blue to visualize the matrix content. Isotype control (B). **ii.** Bone cylinders were treated with repeated washes with hydrogen peroxide for 3 days (H_2O_2-treated; B) to remove the cellular content or maintained in standard culture conditions (control, A) prior to CAM-implantation for 9 days. Relative bone volume changes of individual bone cylinders before and after CAM-implantation measured with µCT; data from 2 independent experiments (H_2O_2-treated) and 6 independent experiments (control) including n=10 per experiment, error bars indicate mean ± SD (C). Following µCT scanning, bone cylinders were processed for Alcian Blue (proteoglycans) and Sirius Red (collagen) histological staining (A-B). Asterisk (*) indicates cell condensation. # indicates bone defect area. Chorioallantoic membrane (CAM), trabecular bone (TB), green fluorescent protein (GFP). Scale bars detailed equivalent to 50 µm (A-D) and 200 µm (E-F).

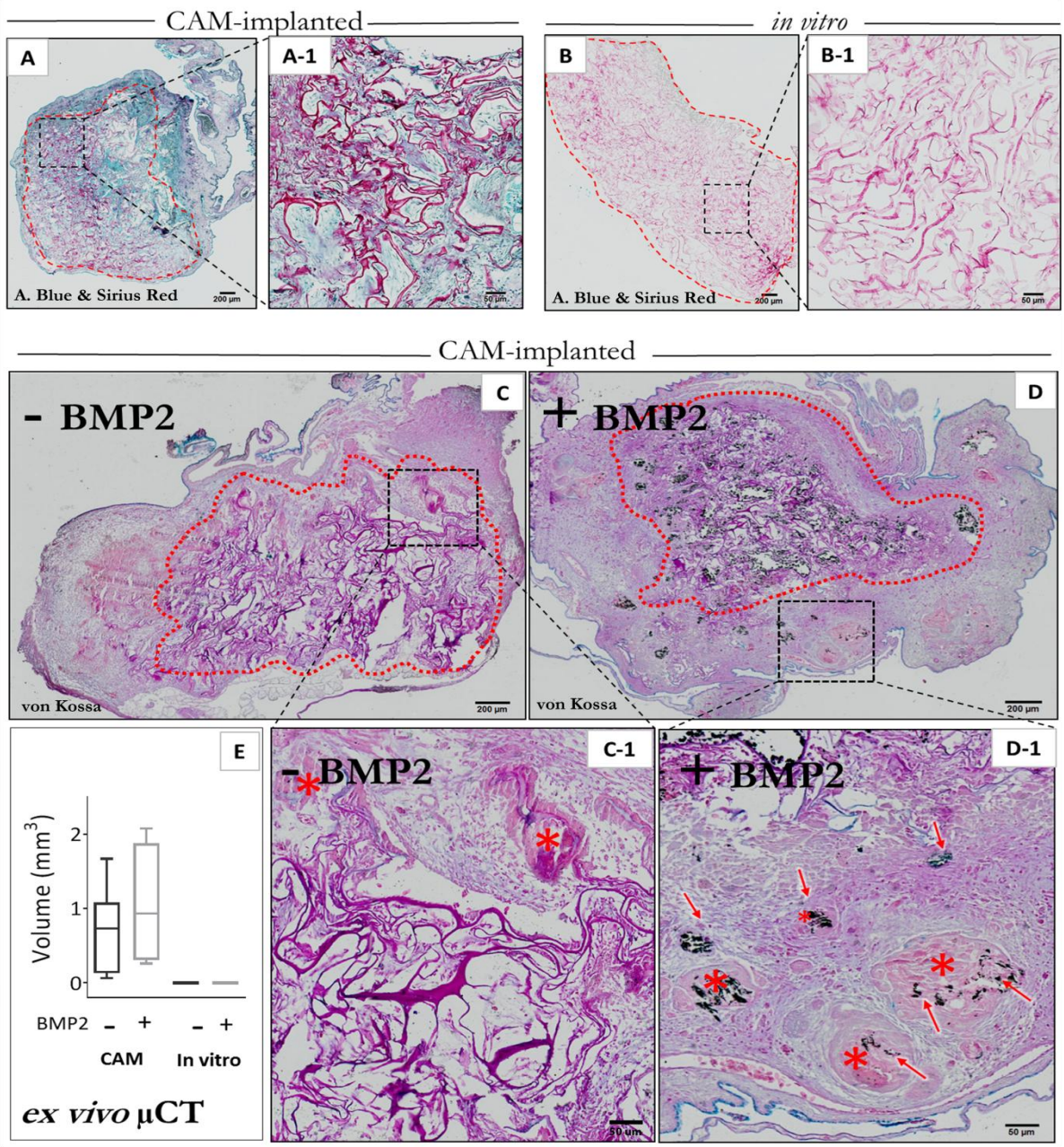

Figure 6: Extracellular matrix and mineral deposition following BMP2 delivery on CAM-implanted acellular collagen sponges (ACS) implanted on CAM. Commercial acellular collagen sponges of standard size containing 0 µg BMP2 (vehicle control; A-A1, B, B-1, C, C-1) or 2.4 µg BMP2 (D, D-1) were implanted on the CAM for 9 days or cultured *in vitro* for 9 days (B, B-1). At harvest, ACS were µCT scanned to quantify mineral deposition (E) and then processed for paraffin histology omitting the decalcification step. Representative images of sections stained for Alcian Blue (proteoglycan) and Sirius Red (collagen) staining (A, A-1, B, B-1). Representative images of sections stained for von Kossa (C, C-1, D, D-1) to display mineral deposition (black), cell cytoplasm (pink), proteoglycans (blue). Dashed line in red indicates the collagen sponge area, asterisks indicate cell condensations, arrows indicate mineral deposition. Scale bars equivalent to 200 µm (A, B, C, D) and 50 µm (A-1, B-1, C-1, D-1). µCT analysis was used to measure the volume of mineralised tissue (mm^3) of the collagen sponges after ± BMP2 treatment followed by *in vitro*-culture or CAM-implantation for 9 days (E). Data collected from 3 independent experiments, n=3-4 per experiment (E).